

Wireless Communications in Tunnels for Urban Search and Rescue Robots^{*}

Kate A. Remley, Galen Koepke,
Dennis G. Camell,
Chriss Grosvenor
NIST Electromagnetics Division
325 Broadway
Boulder, CO, USA 80305
+1 303 497-3652
remley@boulder.nist.gov

Lt. George Hough
New York City Fire Department
New York City, NY USA
gch9@columbia.edu

Robert T. Johnk
Institute for Telecommunications
Sciences
325 Broadway
Boulder, CO, USA 80305
bjohnk@its.bldrdoc.gov

ABSTRACT

We report on propagation tests carried out in a subterranean tunnel to support improved wireless communications for urban search and rescue robots. We describe single-frequency and ultrawideband channel-characterization tests that we conducted, as well as tests of telemetry and control of a robot. We utilize propagation models of both single-frequency path loss and channel capacity to predict robot performance. These models can also be used for optimizing wireless communications in tunnels of various sizes, materials, and surface roughness.

Categories and Subject Descriptors

Defining and measuring aspects of an intelligent system.
Evaluating components within intelligent systems

General Terms

Measurement, Performance, Reliability, Experimentation,
Standardization, Verification.

Keywords

Multipath; radiowave propagation; RMS delay spread; robot;
urban search and rescue; wireless communication; wireless
system

INTRODUCTION

Researchers from the Electromagnetics Division of the National Institute of Standards and Technology (NIST) and the Fire Department of New York (FDNY) conducted tests of radiowave transmission and detection in tunnels at the Black Diamond Mines Regional Park near Antioch, California on March 19-21, 2007. Our goal was to investigate propagation channel characteristics that affect the reliability of wireless telemetry and control of Urban Search and Rescue (US&R) robots in tunnels and other weak-signal environments. We describe measurement methods that we used to study parameters relevant to robot performance. We also use the measured data to verify models of radiowave propagation in tunnels. These models can be used to predict robot performance in tunnels having characteristics different from the ones we measured, such as subways and utility tunnels. This work

supports the development of technically sound standards for US&R robots [1-3].

We used both time- and frequency-domain techniques to study issues such as channel multipath and loss that may impede successful wireless communications in tunnels. We tested both video and control of a robot inside a mine tunnel. We also implemented propagation models of path loss and channel capacity and compared our measured results to these models. We summarize below the data we collected and interpret the key findings from the study, which is described in its entirety in [4].

Recently, the wireless field has seen a renewed interest in studies of signal propagation in both mine and subway tunnels, following a good deal of study on mine communications in the 1970s. A seminal work on mine tunnel propagation by Emslie et al. [5], studied radiowave propagation in small underground coal tunnels (4.3 m wide x 2.1 m high) for frequencies ranging from 200 MHz to 4 GHz. Emslie developed a model for propagation in tunnels that is used today. Recently, Rak and Pechak [6] applied Emslie's work to small cave galleries for speleological applications, confirming Emslie's findings that once a few wavelengths separate the transmitter and receiver, the tunnel acts as a waveguide that strongly attenuates signals below the waveguide's cutoff frequency. Because the walls of the tunnel are not perfectly conducting, signals operating above the cut-off frequency also experience significant loss. In a recent paper, Dudley, Lienard, Mahmoud, and Degauque [7] performed a detailed assessment of operating frequency in a variety of tunnels. They found that as frequency increases, the lossy waveguide effect decreases.

Our measurements, covering a much wider frequency range than [7], and implementation of the model of [6] also confirm the lossy waveguide effect in the tunnels we studied. This effect can have a significant impact on choice of frequency for critical applications such as US&R operations, where typically infrastructure such as a repeater network is not available and lives may be at stake.

Another factor in tunnel communications is multipath caused by reflections off the walls, floor, and ceiling of the tunnel. This was clearly seen in the work of Dudley, et al. [7]. Multipath can have a pronounced effect on successful transmission of wideband

^{*}Publication of the U.S. government, not subject to copyright in the U.S.

Permission to make digital or hard copies of all or part of this work for personal or classroom use is granted without fee provided that copies are not made or distributed for profit or commercial advantage and that copies bear this notice and the full citation on the first page. To copy otherwise, or republish, to post on servers or to redistribute to lists, requires prior specific permission and/or a fee.

PerMIS'08, August 19–21, 2008, Gaithersburg, MD, USA.

Copyright 2008 ACM 978-1-60558-293-1...\$5.00

data. Multipath interference may affect certain frequencies in a wideband signal while simultaneously having little impact on other frequencies. This frequency selectivity can make decoding signals difficult for the demodulator in a receiver.

We studied the severity of multipath in the tunnel environment by measuring the RMS delay spread, as well as the success or failure of wideband data transfer by use of a commercially available robot. We compare our measured results to a model of channel capacity based on Shannon’s theory of channel capacity [6]. This theorem provides a basis for predicting the success of wireless communication in multipath environments.

We first describe the measurements we carried out and interpret the results. We then discuss the models we implemented and how they can be used to optimize radio communications for US&R applications.

1. TEST ENVIRONMENT

The Black Diamond Mines are part of an old silica mine complex that was used early in the 1900s to extract pure silica sand for glass production. As such, the walls of the mine shafts are rough and consist of sandy material.

Two tunnels were studied, the Hazel-Atlas North (here called the “Hazel-Atlas” tunnel) and Hazel-Atlas South (here called the “Greathouse” tunnel). The tunnels are located beneath a mountain and are joined together deep inside, as shown in Figure 1(a). The dimensions of the Hazel-Atlas tunnel varied from approximately 1.9 m (6’, 3”) x 1.9 m to as much as 2.6 m (8’, 5”) x 2.4 m (8’, 0”). The dimensions of the Greathouse tunnel were somewhat bigger, up to approximately 3 m square in places. The Hazel-Atlas tunnel contained railroad tracks spaced 61 cm (24”) apart. Both tunnels consisted of a straight section followed by a 90 degree turn around a corner, as shown in Figure 1(a). Below we report on results for the Hazel-Atlas mine tunnel, shown in more detail in Fig. 1(b). The complete set of data on both tunnels can be found in [4].

Figure 2 shows photographs of the tunnel, including: 2(a) the portal (entrance) of the Hazel-Atlas mine; 2(b) approaching the right-angle turn shown in Figure 1(b); and 2(c) past the turn. The photos show the rough, uneven walls in the tunnels, some with wooden shoring, and the railroad tracks.

2. MEASUREMENTS

2.1 Narrowband Received Power

We measured the power received outside the tunnel from a transmitter placed at various locations inside the tunnel. We collected single-frequency (unmodulated, carrier only) received-power data at frequencies near public-safety bands (approximately 50 MHz, 150 MHz, 225 MHz, 450 MHz). Gathering information at these frequencies helps to provide a choice of optimal frequency for the US&R community for this environment, both for robot communications and for other types of radio communication. These data provide insight into the lossy waveguide effect mentioned in the Introduction.

The handheld transmitters we used were radios similar to those of first responders, except they were placed in ruggedized cases and were modified to transmit continuously. Each radio transmitted a signal of approximately 1 W through an omnidirectional “rubber duck” antenna mounted on the case.

During the tests, the radio antennas were approximately 0.75 m from the floor, a height similar to that of the robot we studied.

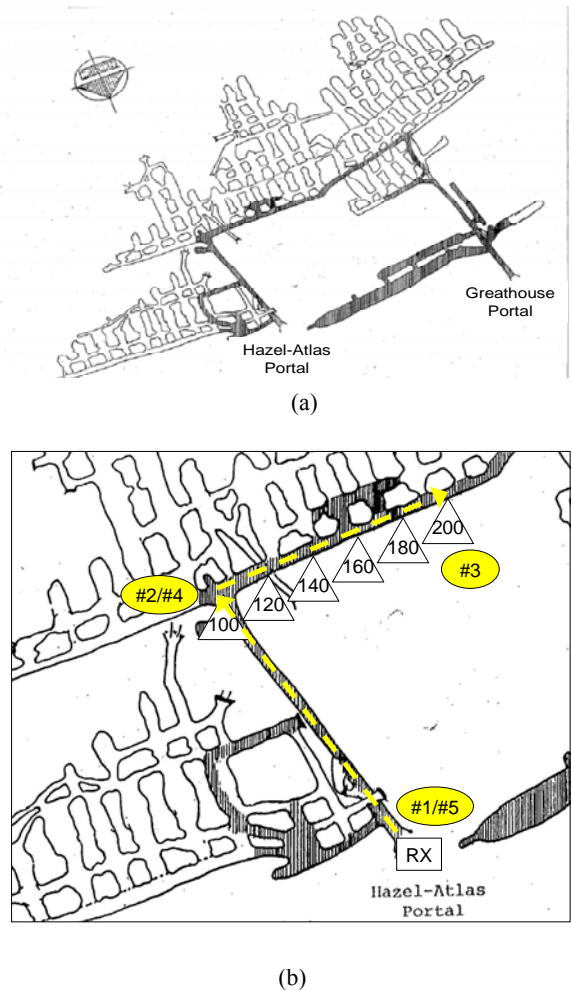


Figure 1: (a) Overview of the Hazel-Atlas mine tunnel complex. The network of mines is located deep within a mountain. The dark-shaded areas are accessible. (b) Close-up view of the Hazel-Atlas tunnel. The dashed line shows the path along which we took measurements, including the right-angle turn at 100 m. The triangles indicate the distance in meters, the ovals correspond to locations shown in Fig. 3, and the receiving equipment is labeled RX.

We carried the radio transmitters from the entrance to locations deep within the tunnels while continuously recording the received signal. From the Hazel-Atlas tunnel portal, we moved the transmitter approximately 100 m down a straight tunnel, then turned a corner and proceeded another 100 m, as shown in Fig. 1(b).

The receiving equipment was located just outside the portal. Omnidirectional discone receiving antennas were mounted on tripods, as shown in Fig. 2(a). We used a narrowband communications receiver to convert the received signal to audio frequencies, where it was digitized by a computer sound card and recorded on a computer. This instrument, when combined with

NIST-developed post-processing techniques [1, 8], provides a high-dynamic-range measurement system that is affordable for most public-safety organizations. Part of the intent of this project was to demonstrate a user-friendly system that could be utilized by US&R organizations to assess their own unique propagation environments.

Figure 3 shows representative measured received-power data at frequencies of 50 MHz, 162 MHz, and 448 MHz acquired while the transmitters were carried by foot through the tunnel. The signals were sampled at approximately 48 kHz and the power averaged over one-second intervals. The left and right halves of the graph show measurements made walking into and out of the tunnel, respectively, and thus mirror each other. The vertical dashed lines on the graph correspond to the entrance (#1, #5), turn (#2, #4), and turn-around point (#3) in the measurement path, as shown in Fig. 1(b).

The cut-off frequency for this type of tunnel is difficult to define since the walls behave as lossy dielectrics rather than conductors. These conditions are discussed in [9], where the attenuation constant is found to vary as the inverse of frequency squared [Section 2.7, pp. 80-83]. Hence, we would expect higher attenuation at the lower frequencies but no sharp cut-off. Further complications in this tunnel are the axial conductors (cables, water pipes, rails) that may support a TEM-like mode of propagation, the irregular cross-section, and the side chambers and tunnels.

For the Hazel-Atlas mine tunnel, we see in Fig. 3(a), strong attenuation of the 50 MHz signal and in Fig. 3(b), the received power of the 162 MHz signal also decreases rapidly as the transmitter moves into the tunnel. This rapid attenuation is due to the lossy waveguide effect described in references [4-7]. The signal for the 448 MHz carrier frequency (Fig. 3(c)) exhibits less attenuation and this is where the models of [5] may apply. Signals may travel even further at higher frequencies, as discussed in [5-7]. This frequency dependence may play a significant role in deciding which frequencies to utilize in US&R robot deployment applications, as will be discussed in Section 3.

2.2 Excess Path Loss and RMS Delay Spread

We also conducted measurements at several stationary positions covering a very wide frequency band. These “excess-path-loss” measurements provide the received signal power relative to a direct-path signal over a frequency band. When transformed to the time domain, the wide frequency band yields a short-time-duration pulse. This pulse can be used to study the number and duration of multipath reflections in an environment.

Our synthetic-pulse, ultrawideband system is based on a vector network analyzer (VNA). Our measurements covered frequencies from 25 MHz to 18 GHz. The post-processing and calibration routines associated with it were developed at NIST [10]. In the synthetic-pulse system, the VNA acts as both transmitter and receiver. The transmitting section of the VNA sweeps over a wide range of frequencies a single frequency at a time. The transmitted signal is amplified and fed to a transmitting antenna. For this study, we used omnidirectional discone antennas for frequencies between 25 MHz and 1.6 GHz, and directional horn-type transmitting and receiving antennas for frequencies between 1 GHz and 18 GHz.



(a)



(b)



(c)

Figure 2: (a) Portal into the Hazel-Atlas mine tunnel. (b) 90 m inside showing the bend depicted in Fig. 1(b) and the rough, sandy wall material. (c) Wood shoring approximately 150 m into the tunnel. The robot we tested can be seen on the cart between the railroad tracks.

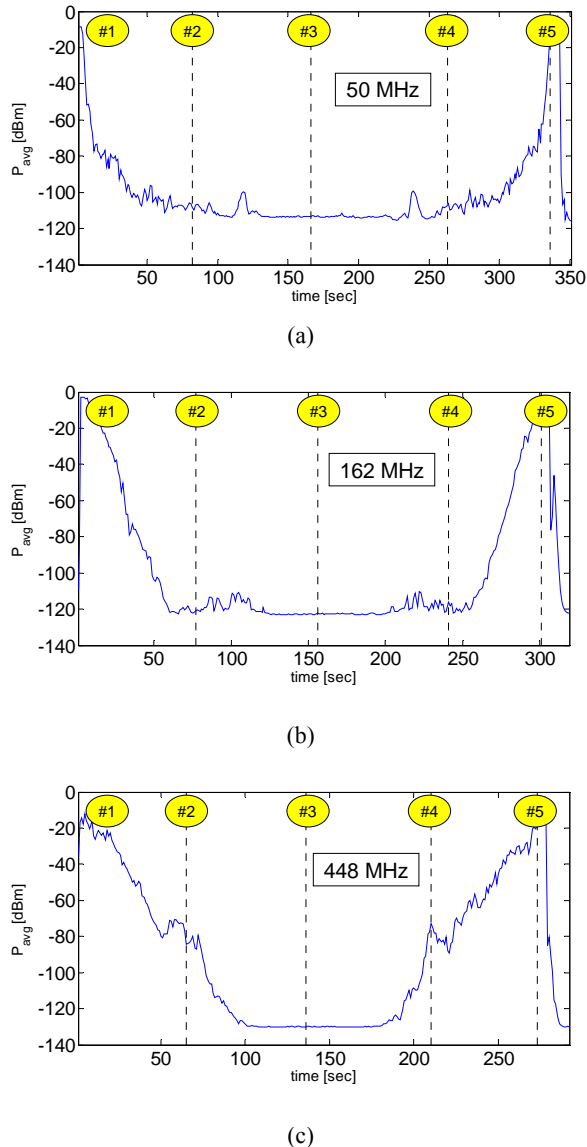


Figure 3: Received-power data in the Hazel-Atlas Mine for three carrier frequencies: (a) 50 MHz, (b) 162 MHz, (c) 448 MHz. In each case the #2 and #4 vertical dashed lines correspond to the turn at 100 m: once on the way into the tunnel and once on the way out. The #3 dashed line represents the end point at 200 m, shown in Fig. 1(b).

The received signal was picked up over the air in the tunnel by the receiving antenna and was relayed back to the VNA via a fiber-optic cable. The fiber-optic cable phase-locks the received signal to the transmitted signal, enabling post processing reconstruction of the time-domain waveform associated with the received signal. The broad range of frequencies and time-domain representation provide insight into the reflective multipath nature of the tunnel that cannot be captured by use of single-frequency measurements. The receive antenna must remain fixed during each measurement, so these tests are carried out at discrete locations, unlike the single-frequency tests.

We measured excess path loss every 20 m starting approximately 10 m into the tunnel. The VNA was located at the Hazel-Atlas portal. The transmitting antenna was located at the portal as well. The graphs show data starting from 0 Hz, however the valid (calibrated) measurement range is stated for each graph.

Figures 4 and 5 show measured excess path loss over a wide frequency band measured 50 m and 120 m, respectively, in the Hazel-Atlas tunnel. Note that at 120 m, we have passed the right-angle turn in the tunnel. The top curve in each graph represents the received power level, referenced to the calculated free-space path loss at that location. The bottom curve represents the noise floor of the measurement system.

Figure 4 shows that even in a line-of-sight condition approximately 50 m from the tunnel entrance, the spectrum of the received signal displays significant frequency dependence. At frequencies between 25 MHz and 1.6 GHz (Fig. 4(a)), the lossy waveguide effect is shown by the rapidly decreasing signal on the left-hand side of the graph. We see that a carrier frequency higher than approximately 700 MHz would suffer less loss compared to lower frequencies in this particular tunnel. Figure 4(b) shows frequencies from 1 GHz to 18 GHz. In this case, we see frequency dependence in received power caused by strong reflections, as shown by the deep nulls and peaks in the top curve of Fig. 4(b).

Once the receiving antenna turns the corner, see Fig. 5, the signal takes on a more random variation with frequency since transmission consists of reflected signals only. For frequencies from 25 MHz to 1.6 GHz (Fig. 5(a)), the received signal power is near the noise floor of the receiver since the two curves almost overlay. For the higher frequencies (Fig. 5(b)), we see that the average received signal level is relatively constant with frequency, but the peaks and nulls are still significant.

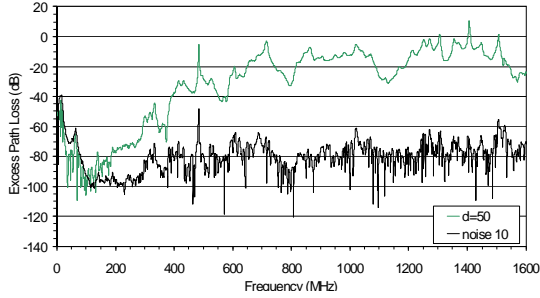
Finally, we present the RMS delay spread for the Hazel-Atlas mine tunnel in Table 1 for frequencies from 25 MHz to 1.6 GHz and 1 GHz to 18 GHz. We see that the shortest delay spreads are found by use of the directional antennas. The complete set of UWB excess-path-loss data is given in [4].

2.3 Tests of Robot Communications

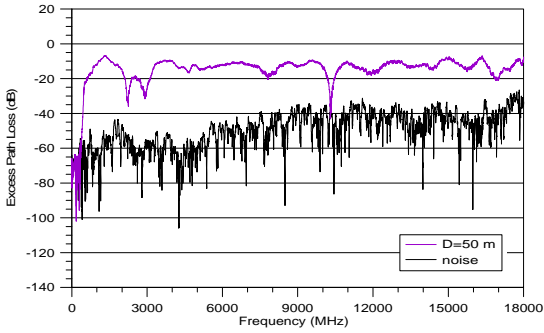
We carried out tests on a commercially available robot. Control and video were as-built for the commercial product. We used the omnidirectional antennas that came with the system for all tests in order to assess the default capabilities of this robot.

The robot we used is controlled with a 2.4 GHz spread-spectrum, frequency-hopping protocol, which was configured to transmit in the unlicensed 2.4 GHz industrial, scientific, and medical (ISM) band. The control channel utilizes a modulation bandwidth of approximately 20 MHz. The output power of the bidirectional control link is nominally 500 mW.

The robot transmits video by use of one of ten channels between 1.7 GHz and 1.835 GHz. The robot we tested transmitted at 1.78 GHz by use of an analog modulation format that was non-burst and non-frequency-agile. The video channel utilized approximately 6 MHz of modulation bandwidth. The output power was nominally 2 watts.

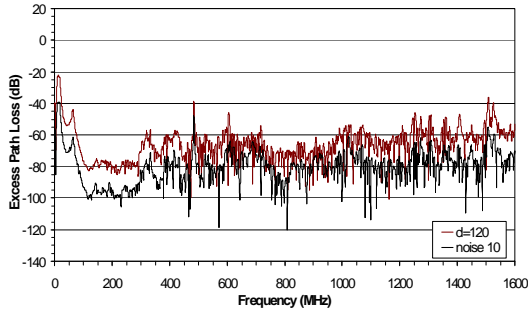


(a)

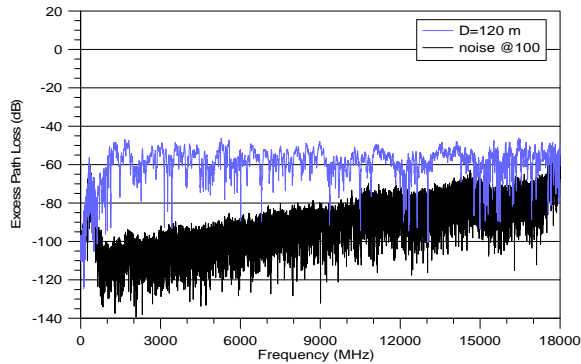


(b)

Figure 4: Excess path loss measurements over a wide frequency band carried out 50 m from the portal of the Hazel-Atlas mine. (a) 25 MHz to 1.5 GHz. (b) 1 GHz to 18 GHz.



(a)



(b)

Figure 5: Excess path loss measurements carried out 120 m from the portal of the Hazel-Atlas mine. (a) 25 MHz to 1.6 GHz. (b) 1 GHz to 18 GHz.

Table 1: RMS Delay Spread for the Hazel-Atlas mine tunnel. Center column: Frequencies from 25 MHz to 1.6 GHz measured with omnidirectional antennas. Right column: Frequencies from 1 GHz to 18 GHz measured with directional antennas. The gray-shaded areas represent a non-line-of-sight propagation condition.

Distance (m)	RMS Delay Spread Low Freqs. (ns)	RMS Delay Spread High Freqs. (ns)
0	31.0	14.4
10	25.3	17.6
20	18.5	7.6
30	15.9	15.0
40	17.0	11.5
50	15.5	13.1
60	19.7	20.6
70	17.2	11.1
80	15.2	10.0
90	15.2	8.4
100	15.7	9.6
110	x	7.5

The robot controller was located at the entrance to the tunnel, shown in Fig. 6. We positioned the robot inside the tunnel after the first bend in a non-line-of-site condition. The robot was moved through the tunnel on a cart, as shown in Fig. 2(c), so that we could check the control link even after video was lost. Every 10 m, the video quality and control link were checked. Video was rated qualitatively by the robot operator, and control was checked by the ability of the operator to move the robot arm, and verified by a researcher in the tunnel. No attempt was made to provide more granularity in these tests. That is, we assumed that moving the arm up was equivalent to moving it down or rotating it.

Table 2 shows the results of our tests. We were able to communicate with the robot in a non-line-of-sight condition deep within the tunnel. This is consistent with the results of Fig. 5(b), which indicates that signals in the low gigahertz range should propagate farther than those at lower frequencies.

Table 2 also shows that control of the robot was possible much deeper into the tunnel than we were able to receive video, even though the output power of the video channel is higher (2 watts for video vs. 0.5 watt for control). However, a much higher data rate is necessary to maintain high-quality video transmission, as opposed to the relatively small amount of data needed to control the robot. Transmitting this large amount of data requires a more stringent success rate than for the control channel; therefore, failure of the video before the control is not unexpected. The delay experienced in controlling the robot when it was deep in the mine indicates packet loss and resend for error correction under weak-signal conditions.



Figure 6: Robot operator positioned at the entrance to the Hazel-Atlas mine tunnel. The robot was operated in a non-line-of-sight condition more than 100 m inside the tunnel.

Table 2: Results of wireless communication link tests carried out inside Hazel-Atlas tunnel at Black Diamond Mines Regional Park.

Distance in tunnel (m)	Video quality (1.7 GHz)	Control of arm (2.4 GHz)
100	good	yes
110	good	yes
120	poor (intermittent)	yes
130	poor (intermittent)	yes
140	very poor	yes
150	none	yes
160	none	delay experienced
170	none	intermittent control
180	none	delay experienced
190	none	delay experienced
200	none	delay experienced
205	none	none

3. MODELED RESULTS

3.1 Single-Frequency Path Gain Models

To study the extent of waveguiding in these tunnels, we implemented an analytical model that simulates signal propagation in tunnel environments having various physical parameters [5, 6, 11]. Briefly, the model assumes a dominant EH_{11} mode in a lossy rectangular waveguide with the attenuation α in dB/m expressed for vertical polarization as

$$\alpha = \alpha_{\text{TUNNEL}} + \alpha_{\text{ROUGHNESS}} + \alpha_{\text{TILT}}, \quad (1)$$

where

$$\alpha_{\text{TUNNEL}} = 4.343\lambda^2 \left(\frac{1}{a^3 \sqrt{\epsilon_R - 1}} + \frac{\epsilon_R}{b^3 \sqrt{\epsilon_R - 1}} \right), \quad (2a)$$

$$\alpha_{\text{ROUGHNESS}} = 4.343\pi^2 h^2 \lambda \left(\frac{1}{a^4} + \frac{1}{b^4} \right), \quad (2b)$$

$$\alpha_{\text{TILT}} = 4.343 \frac{\pi^2 \theta^2}{\lambda}, \quad (2c)$$

and λ is the wavelength, a is the width of the tunnel, b is the height of the tunnel, and h is the roughness, all in meters. Other parameters include ϵ_R , the dielectric constant of the rock walls, and θ , the angle of the tunnel-floor tilt in degrees.

We set the parameters of the model to approximate the Hazel-Atlas tunnel, given below in Table 3. This model works well only for frequencies will above the cut-off frequency, that is, for wavelengths significantly less than the dimensions of the tunnel [5, 6]. Hence, in Fig. 7 we show results for 448 MHz only. At distances around 80 m, the signal was able to propagate through an air vent as well as through the tunnel, so the overall received signal level increases. The good agreement between the measured and modeled data led us to conclude that waveguiding plays a significant role in radio propagation in these tunnels.

Table 3: Parameters used in tunnel model.

Parameter	Value
Width	2 m
Height	2 m
Wall roughness	0.3
ϵ_r	6
tilt	1°

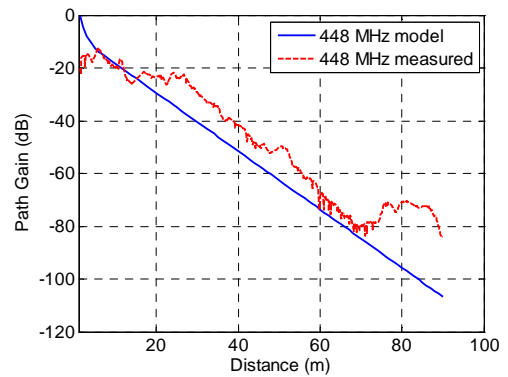


Figure 7: Comparison of measured and modeled data for the Hazel-Atlas tunnel. The carrier frequency is 448 MHz. The modeled data simulate waveguide propagation for a waveguide whose physical parameters approximate those of the tunnels.

The model also lets us explore which frequencies may be optimal for robot or other wireless communications in the tunnel. Figure 8 compares a number of commonly used emergency

responder frequencies as a function of distance within the tunnel. As discussed in [5, 6], the frequency-dependent behavior of the tunnel leads to a “sweet spot” in frequency. Below the sweet spot, signals do not propagate well, due to the effect of waveguide-below-cutoff attenuation and wall loss. Above the sweet spot, free-space path loss (which increases with frequency) and α_{TILT} dominate and signals do not propagate well. Again, models such as these may enable a choice of appropriate frequency for US&R robot communications in tunnel environments. Note that these results are valid only for a tunnel with these dimensions, wall materials, and surface roughness. The curves would need to be recalculated for other types of tunnels.

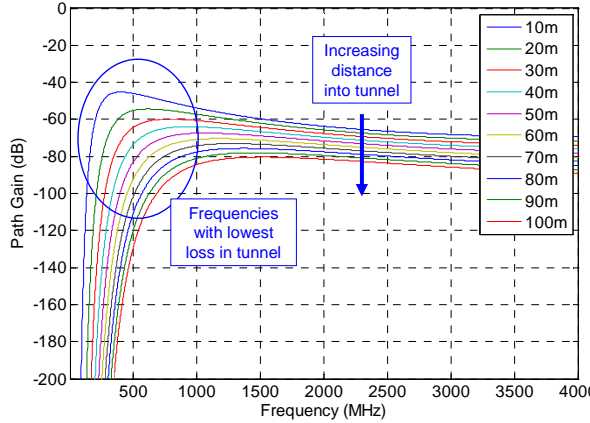


Figure 8: Path gain versus frequency for various distances in a tunnel having physical characteristics similar to those of the Hazel-Atlas tunnel. Frequencies around approximately 400 MHz to 1 GHz propagate better than either lower or higher carrier frequencies.

We also used the model to investigate the video performance of the robot, described in Section 3.c. The frequency-hopping control channel would need to be modeled by use of other methods, since it consists of several narrowband channels frequency hopping within a wide modulation bandwidth. In Fig. 9, we plot the estimated path gain at a carrier frequency of 1.78 GHz for the tunnel environment with a right-angle turn 100 m from the receiver. We used the parameters in Table 3 for the model. A path gain of -40 dBW was used as an approximation for the turn in the tunnel at 100 m, based on work done by Lee and Bertoni in [12]. We plot the flat earth path gain for comparison.

Figure 9 also shows the theoretically computed excess link margin (ELM). The ELM is the difference between the received signal strength and the minimum receiver sensitivity. The receiver sensitivity is determined by the thermal noise of the receiver and the receiver’s front-end amplifier noise (5 dB, as a rule of thumb). The thermal noise is given by $N = kTB$, where k is the Boltzmann constant, T is the temperature in Kelvin, and B is the bandwidth of the receiver. In order for a wireless link to be maintained, the ELM must be greater than zero dB.

The ELM plotted in Fig. 9 agrees well with the measured results from Table 2, which show that the video completely drops out between approximately 140 m and 150 m. Given the fluctuation in signal strength due to multipath fading in this tunnel environment, once the link margin drops below 10 dB at

approximately 120 m, the video quality degrades and the picture becomes intermittent.

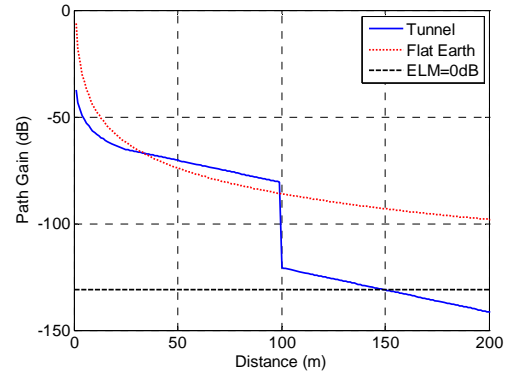


Figure 9: Path gain curves for tunnel with a right-angle turn at 100 m (solid) and flat earth (dashed) environments. The curve labeled “ELM = 0” indicates where the excess link margin calculation predicts loss of signal. As shown, this occurs approximately 150 m into the tunnel.

3.2 Channel Capacity Model

In general, received RF power and bandwidth effectively place an upper bound on the capacity of a communications link. The Shannon channel capacity theorem [13] can be used to predict the approximate maximum data rate for tunnel communications, even though the Shannon theorem is based on the assumption of a Gaussian noise (low multipath) environment. For a given modulation bandwidth, the received signal power relative to the noise power determines the theoretical upper limit on the data rate (channel capacity). The Shannon capacity theorem is given by

$$C = B \log_2(1 + S/N), \quad (3)$$

where C is the channel capacity in bits/second, B is the channel bandwidth in hertz, S is the received signal power in watts, and N is the measured noise power in watts. The capacity represented by this equation is the upper limit, and in reality the capacity would be difficult to attain with real hardware.

For an analog transmission, Shannon’s limit gives us a way to estimate the channel capacity. The National Television System Committee (NTSC) analog video channel that our robot used has a video bandwidth of 4.2 MHz and a transmission rate of approximately 30 frames per second, where each frame consists of 525 scanning lines, giving a line rate of 15.734 kHz [14]. We can place an upper bound on the amount of data that could be transmitted in each line by considering a typical implementation of NTSC, where each line is digitized into 768 pixels. This gives a digital scanning rate of approximately 12 MHz. The specification of 768 pixels per line is used in studio environments. We expect the potential channel capacity to be lower in the analog transmission case.

Figure 10 shows simulations of the Shannon limit for our robot’s 4.2 MHz video bandwidth, 1.78 GHz video channel. Table 4 shows the distance into the tunnel where 12 Mb/sec transmission rate occurs assuming our maximum possible channel

capacity to be various fractions of the Shannon limit. Based on this information, we would expect to encounter video problems somewhere between 120 m and 130 m into the tunnel, which Table 2 shows is indeed where we started to experience signal degradation. Thus, we are able to form a rough estimate of the distance into the tunnel where we expect the video to fail based on a simple implementation of the Shannon theorem.

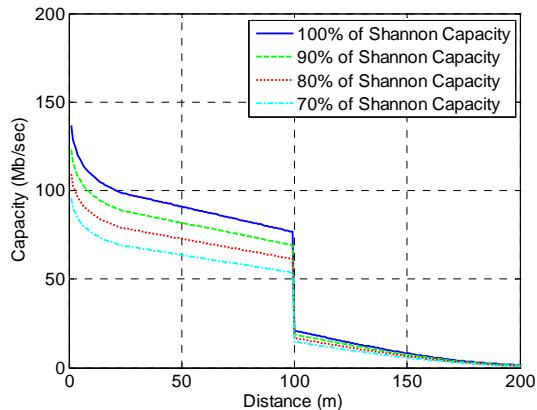


Figure 10: Channel capacity predicted by the Shannon theorem for a carrier frequency of 1.78 GHz and a video modulation bandwidth of 4.2 MHz. At 120 m, where we experienced intermittent video, 80 % of the Shannon limit is 15.4 Mb/sec and 70 % of the Shannon limit is 13.5 Mb/sec.

Table 4: Distance into tunnel for a channel capacity of approximately 12 Mb/sec.

Fraction of Shannon capacity (%)	Distance into tunnel (m)
100	133
90	129
80	122
70	114

4. CONCLUSION

We have presented measured data collected in a subterranean tunnel environment. Results showed waveguide-below-cutoff and wall attenuation effects. We saw frequency-dependent peaks and nulls in the channel due to strong multipath reflections and attenuation in the tunnel. In non-line-of-sight conditions, we saw classic Rayleigh-distributed noise-like signals.

We implemented models that may be used to predict radiowave propagation and modulated-signal performance within tunnels for robots or other wireless devices. Using the models, it was possible to ascertain the optimal carrier frequency range for a robot within this tunnel environment. The intent of this work is to improve radio communications for urban search and rescue robots when they transmit wideband, digitally modulated signals. We hope that these data will prove useful in standards development,

as well as improved technology and system design for the emergency-responder community.

5. ACKNOWLEDGEMENT

The authors thank Alex Bordetsky of the Naval Postgraduate School for facilitating the measurements during recent interagency marine interdiction operation system tests. We also thank Bill Dunlop, Steve MacLaren, and Dave Benzel of Lawrence Livermore National Laboratory for logistical and technical support. We are indebted to Frederick M. Remley for details on the NTSC video standard.

6. REFERENCES

- [1] Elena Messina, "Performance Standards for Urban Search and Rescue Robots," *ASTM Standardization News*, August 2006, http://www.astm.org/cgi-bin/SoftCart.exe/SNEWS/AUGUST_2006/messina_aug06.html.
- [2] National Institute of Standards and Technology, "Statement of Requirements for Urban Search and Rescue Robot Performance Standards-Preliminary Report" [http://www.isd.mel.nist.gov/US&R_Robot_Standards/Requirements%20Report%20\(prelim\).pdf](http://www.isd.mel.nist.gov/US&R_Robot_Standards/Requirements%20Report%20(prelim).pdf)
- [3] K. A. Remley, G. Koepke, E. Messina, A. Jacoff, G. Hough, "Standards development for wireless communications for urban search and rescue robots," *Proc. Int. Symp. Advanced Radio Technol.*, pp. 66-70, Boulder, CO, Feb. 2007.
- [4] K.A. Remley, G. Koepke, C.L. Holloway, C. Grosvenor, D. Camell, J. Ladbury, D. Novotny, W.F. Young, G. Hough, M.D. McKinley, Y. Becquet, J. Korsnes, "Measurements to support broadband modulated-signal radio transmissions for the public-safety sector," *Natl. Inst. Stand. Technol. Note 1546*, Apr. 2008.
- [5] A.G. Emslie, R.L. Lagace, and P.F. Strong, "Theory of the propagation of UHF radio waves in coal mine tunnels," *IEEE Trans. Antennas and Prop.*, vol. 23, no. 2, Mar. 1975, pp. 192-205.
- [6] M. Rak and P. Pechac, "UHF propagation in caves and subterranean galleries," *IEEE Trans. Antennas and Prop.*, vol. 55, no. 4, April 2007, pp. 1134-1138.
- [7] D. G. Dudley, M. Lienard, S.F. Mahmoud and P. Degauque, "Wireless propagation in tunnels," *IEEE Antennas Prop. Mag.*, vol. 49, no. 2, April 2007, pp. 11-26.
- [8] M. Rütshlin, K. A. Remley, R. T. Johnk, D. F. Williams, G. Koepke, C. Holloway, A. MacFarlane, and M. Worrell, "Measurement of weak signals using a communications receiver system," *Proc. Intl. Symp. Advanced Radio Technol.*, Boulder, CO, March 2005, pp. 199-204.
- [9] P. Delogne, "Leaky Feeders and Subsurface Radio Communications," IEE press, 1982.
- [10] B. Davis, C. Grosvenor, R.T. Johnk, D. Novotny, J. Baker-Jarvis, M. Janezic, "Complex permittivity of planar building materials measured with an ultra-wideband free-field antenna measurement system," *NIST Journal of Research*, Vol. 112, No. 1, Jan.-Feb., 2007, pp. 67-73.
- [11] G. Hough, "Wireless robotic communications in urban environments: issues for the fire service," Thesis, Naval Postgraduate School, March 2008. http://theses.nps.navy.mil/08Mar_Hough.pdf
- [12] J. Lee and H. Bertoni, "Coupling at cross, T, and L junctions in tunnels and urban street canyons," *IEEE Trans. Antennas Prop.*, vol. 51, no. 5, May 2003, pp. 926-935.
- [13] C.E. Shannon, "Communication in the presence of noise," *Proc. IRE*, vo. 37, no. 1, Jan. 1949, pp. 10-21.
- [14] C.A. Poynton, "A Technical Introduction to Digital Video," Wiley, 1996, pp 26-27.